

INTERNATIONAL JOURNAL OF CHEMICAL REACTOR ENGINEERING

Volume 1

2003

Article A43

Formulation of Reduced-Order Models for the Dynamic and Stability Analyses of Autothermal Radial Flow Reactors

Malte Bartels* Jorge E. Gatica[†] Marisa Pedernera[‡]
Noemí Susana Schbib** Daniel Oscar Borio^{††}

*Dept. of Chem. and Biomed. Eng., Cleveland State University, USA, maltebartels@gmx.net

[†]Dep. of Chem. and Biomed. Eng., Cleveland State University, USA, j.gatica@csuohio.edu

[‡]Dep. of Chem. Eng., PLAPIQUI (U.N.S.-CONICET), Argentina, marisape@posta.unizar.es

**Dep. of Chem. Eng., PLAPIQUI (U.N.S. - CONICET), Argentina, sschbib@plapiqui.edu.ar

^{††}Dep. of Chem. Eng., PLAPIQUI (U.N.S.-CONICET), Argentina, dborio@plapiqui.edu.ar

ISSN 1542-6580

Copyright ©2003 by the authors.

All rights reserved. No part of this publication may be reproduced, stored in a retrieval system, or transmitted, in any form or by any means, electronic, mechanical, photocopying, recording, or otherwise, without the prior written permission of the publisher, bepress, which has been given certain exclusive rights by the author.

Formulation of Reduced-Order Models for the Dynamic and Stability Analyses of Autothermal Radial Flow Reactors

Malte Bartels, Jorge E. Gatica, Marisa Pedernera, Noemí Susana Schbib, and Daniel Oscar Borio

Abstract

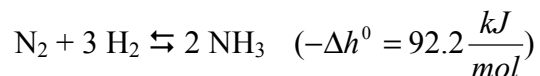
Autothermal radial flow reactors typically consist of a reactor setup of multiple catalyst-beds with internal heat exchange. These reactors are widely used because of their high efficiency due to the internal heat exchange, and radial flow arrangements are preferred due to their low pressure drops. Although an efficient multi-functional reactor arrangement, this setup has shown to provide for an additional destabilizing mechanism via the heat feedback. Thus, additional stability considerations are necessary when operating autothermal or non-adiabatic reactors at high conversions. This work proposes the formulation of a simplified model to investigate the effect of the heat transfer feedback on the stability of autothermal radial flow reactors. The present work focuses on a lumping approach to reduce the order of a complex distributed parameter system. The model is complex enough so as to preserve the intricacies of this reactor arrangement, but still yield a tractable dynamic formulation. The industrial ammonia synthesis process has been chosen as a case study to illustrate the proposed methodology. The lumped model predictions are qualitatively compared against numerical simulations of a detailed mathematical model.

KEYWORDS: autothermal reactors, ammonia synthesis, radial flow, reduced-order model, stability analysis

1. INTRODUCTION

1.1 Autothermal radial flow reactors

This work will focus on the analysis of exothermic, reversible, gas-phase catalytic reactions. Although many industrial processes fall under these headings, an important industrial process with serious equilibrium limitations is the ammonia synthesis via the Haber-Bosch process, i.e.



This process has been selected as a case-study for this paper. Since the synthesis of ammonia proceeds through an exothermic process it is seriously restricted by equilibrium limitations at high temperature. Although an increase in the temperature increases the rate of reaction, it also imposes more stringent equilibrium limitations. As reviewed by Strelzoff (1981), different strategies can be employed to resolve this dilemma: Direct quenching of reacting gas with fresh synthesis gas, cooling of the reactants by external cooling, and heat exchange with the reacting gases. For practical reasons, it has become a common industrial practice to utilize coupled heat exchange mechanisms by combining multiple reactors with heat exchangers. Indeed, due to the cooling of the reactants, a higher conversion becomes possible; simultaneously the new arrangement is more energy efficient by providing the energy needed. The application of heat exchange for increased conversion in reactor arrangements has been extensively investigated in the literature (cf. Abashar, 2000).

The term "autothermal" commonly relates to the presence of one or more heat exchangers between reactors, which provide the preheating of the reactants via heat exchange with the products. This energetic integration is often achieved by a modular system with external heat exchangers. In modern reactors the integration is more frequently realized with internal heat exchangers between beds, with the whole arrangement built completely within a single pressure shell. Since the internal heat exchangers are much more efficient than external ones, this type of reactor arrangement is very popular in industrial practice.

The scientific literature is abundant in descriptions of different types of industrial reactors that resort to intricate heat exchange arrangements to maximize or increase process efficiency (Slack and James, 1977; Vancini, 1971; Strelzoff, 1981). A comprehensive overview of various autothermal fixed-bed reactor concepts has been presented in a recent review by Kolios et al. (2000).

Modern reactor arrangements also often resort to radial flow patterns to increase process efficiency. The shorter pathway for the reactants leads to lower pressure drops. Since pressure drop is commonly associated to significant consumption of energy, considerable economical and ecological improvements can be achieved by adopting radial flow arrangements.

The essential part of a radial flow reactor is the annular arrangement of the porous catalytic bed. This packed-bed of catalyst particles is illustrated in Figure 1 where flow is assumed to occur in the radial direction only. The gaseous reactants can flow either in a centripetal (CP, from the outside in) or centrifugal (CF, from the inside out) mode.

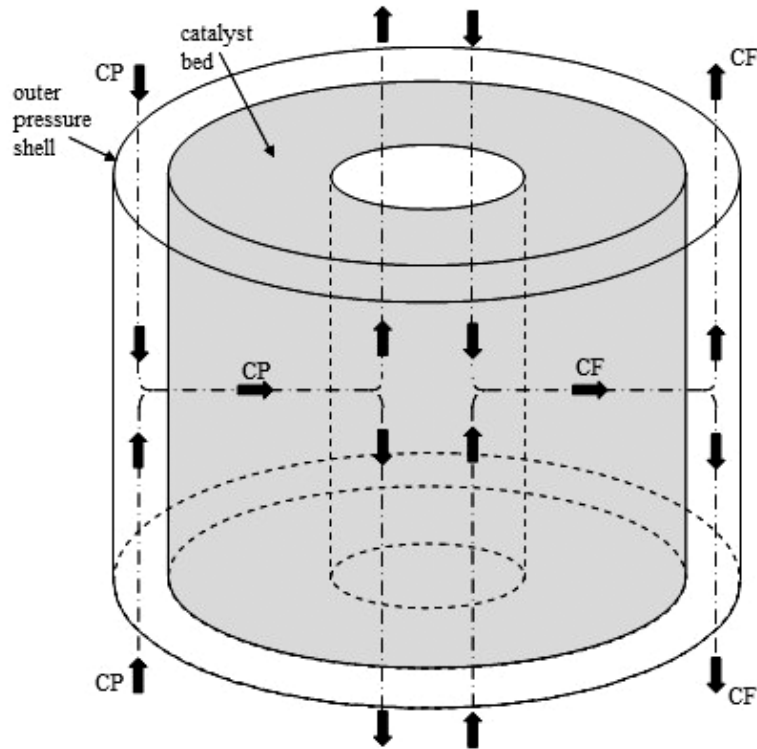


Figure 1: Schematic of a radial flow packed-bed reactor

One widely used radial-flow reactor in ammonia plants is the Haldør Topsoe[®] S-200 (cf. Ullmann's Encyclopedia, 1993), a highly efficient converter. The Haldør Topsoe[®] S-200 is chosen as an example for this study because of its frequent application in many large ammonia plants. Since the original introduction of the S-200 series in 1976 this converter type has been used in more ammonia plants than any other competing converter design. This reactor is produced in two different configurations, the flow sheet for both versions of this reactor is presented Figure 2.

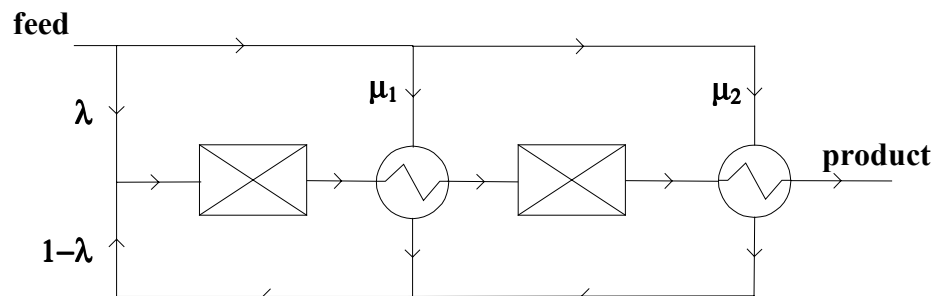


Figure 2: Flow sheet of a two-bed reactor with one inter-bed heat exchanger and an optional ("lower") heat exchanger after the second bed

The reactor always includes the so-called "inter-bed" heat exchanger between both beds. Optionally, a second heat exchanger after the second bed can be included. Given the geometrical setup of the actual reactor, this heat exchanger will be referred to as the "lower" heat exchanger for the remainder of this paper. Both configurations will be investigated. These additional mechanisms for energy feedback lend this system a potential for unstable behavior. As shown in the work by Morud and Skogestad (1998), instabilities can occur in operating ammonia plants, resulting in wide temperature oscillations with the subsequent catalyst damage or deactivation. From this

observation it becomes clear that operation and control strategies demand a-priori information about the stability of the system. A model of the reactor from which general conditions for stability can be drawn will then be useful in predicting unstable behavior or safe operating windows.

1.2 Previous research

Different autothermal reactor setups have been investigated in the past. Bildea et al. (2001), for instance, investigated the multiplicity and stability behavior of a heat-integrated multitubed plug-flow reactor. They observed different regions of behavior in the state space, including oscillatory behavior for realistic model parameters.

Another approach to this reactor design can be found in the contribution by Kienle et al. (1995). These authors investigated a circulation loop reactor (CLR), which is intended as an autonomous periodic system. The principle of the CLR is based on self-exciting travelling reaction zones. Their work showed that this reactor has a rich dynamic and steady-state behavior with a large region of parameters for the desired periodic regime.

Radial flow reactors were early modeled by Hlavacek and Kubicek (1972), who derived a one-dimensional model for radial-flow reactors and identified the necessary conditions for multiplicity for first-order kinetics. However, a first-order kinetic is not sufficient for the ammonia synthesis reaction, since it operates at high temperatures and pressures where the reverse reaction becomes important and serious equilibrium limitations are observed.

Pedernera et al. (1999) presented a more detailed steady-state heterogeneous model for radial flow reactors and analyzed the ammonia synthesis reaction. This model is quite complex, thus leading to more detailed information on the temperature profiles, but its complexity makes it impractical for operation- and control applications.

Morud and Skogestad (1998) analyzed an idealized configuration for a multi-bed industrial ammonia reactor, and identified the presence of conditions leading to rapid temperature oscillations. Utilizing a dynamic stability rather than a steady-state analysis, they found that a pair of complex conjugate poles crosses the imaginary axis introducing the unstable behavior. Furthermore, they made some recommendations for possible control strategies.

1.3 Motivation for this study and overview of this work

This study proposes a modeling approach of autothermal radial flow reactors by means of a simplified model. The simplified nature of the model is aimed at reducing its mathematical complexity but capable of still capturing the main behavior of the reactor. A reduced-order, or also called "lumped", model of autothermal radial flow reactors for the steady state and dynamic stability analysis has been developed. Reduced-order models are developed in order to keep the computational effort low but retain the lowest degree of complexity that can capture the main behavior of the system correctly.

The term "lumped" is also used in the traditional control terminology to differentiate this model from a distributed parameters system. Specifically in this work the lumping is made in the radial direction, while no axial distribution is assumed. When one examines the final formulation, it becomes apparent that each bed is characterized by a single (parameter) temperature, while a distributed parameters analysis would provide a profile instead. In order to highlight the goodness of the lumped formulation, a comparison between both approaches is included in this paper. The lumping methodology follows the "pseudo-homogeneous" model (Vortmeyer and Schaefer, 1974); i.e. the temperature distributions for both phases, solid and gas, have been "lumped" together and transport properties refer to "effective" parameters instead. Furthermore, this approach follows the analysis of Hlavacek and Kubicek (1972) where the governing equations are approximated by equations in differences.

Despite its simplicity the model is able to predict a range of typical solutions and give more insight into the design of control strategies. In particular, reduced-order models are especially favorable for operation- and control applications. It is worth mentioning here that, since the focus is on the model structure, which allows a fast, real-time evaluation of the model equations, the accuracy of the solution has been considered less significant.

2. MATHEMATICAL MODEL

2.1 Dimensionless Mass and Energy Balances; Boundary conditions

The two most common packed-bed configurations used to overcome pressure drop limitations are radial-flow and spherical reactors. These reactors can be efficiently described by a pseudo-homogeneous model (Vortmeyer and Schaefer, 1974). For the sake of simplicity, the following assumptions are made:

1. Uniformly packed bed, channeling or shortcut-effects through the packed bed of catalyst do not occur
2. The physical properties of the reacting gas (spec. heat capacity, density, etc.) are reasonably described by mean values.
3. Absence of any concentration and temperature gradients within the catalyst particles
4. Absence of any axial and angular temperature and concentration gradients
5. Negligible pressure drop along the bed (constant pressure)
6. Adiabatic operation.

The dimensional form of the steady-state governing equations can be referred to the work of Hlavacek and Kubicek (1972). Formulated in terms of dimensionless parameters (defined in the nomenclature section) they can be written as:

Mass balance:

$$\frac{1}{Pe_M} \left(\frac{d^2 Y}{d\xi^2} + \frac{a}{\xi} \frac{dY}{d\xi} \right) \pm \frac{1}{\xi^a} \frac{dY}{d\xi} = Da \exp\left(\frac{\theta}{1+\theta/\gamma}\right) \hat{r}(Y, \theta) \quad (1)$$

Energy balance:

$$\frac{1}{Pe_H} \left(\frac{d^2 \theta}{d\xi^2} + \frac{a}{\xi} \frac{d\theta}{d\xi} \right) \pm \frac{1}{\xi^a} \frac{d\theta}{d\xi} = -B Da \exp\left(\frac{\theta}{1+\theta/\gamma}\right) \hat{r}(Y, \theta) \quad (2)$$

where the geometry factor "a" is used to formulate a generalized equation applicable to tubular (0), radial flow (1), and spherical (2) reactors. In both equations the upper sign in the convective term (\pm) refers to centripetal (CP) flow while the lower one corresponds to centrifugal (CF) flow.

In contrast to the original work of Hlavacek and Kubicek (1972) the expression for the reaction rate is taken from the work of Temkin and Pyzhev (1940):

$$\omega_{N_2} = \frac{dp_{N_2}}{dt} = \frac{1}{\rho_{cat}} \left(k_1 * p_{N_2} * \left(\frac{p_{H_2}^3}{p_{NH_3}^2} \right)^{order} - k_2 * \left(\frac{p_{NH_3}^2}{p_{H_2}^3} \right)^{(1-order)} \right) \quad (3)$$

where p_i are the partial pressures of each component i , k_1 and k_2 are rate constants for synthesis and decomposition and "order" is a catalyst-dependent constant (here order=0.5). Through the assumption of constant total pressure, an exponential of the total pressure ($p_T^{(1+order)}$) is an integral part of the definition for the Damköhler number, Da , yielding the dimensionless formulation of the reaction rate shown in Equation (4).

$$\hat{r}(Y, \theta) = \left[y_A \left(\frac{y_B^3}{y_C^2} \right)^{0.5} - \frac{1}{K} p_T^{-2} \left(\frac{y_C^2}{y_B^3} \right)^{0.5} \right] \quad (4)$$

The boundary conditions utilized with the governing equations are chosen according to Danckwerts (1953), i.e. a discontinuity in the temperature/concentration profiles at the inlet of the bed (closed-closed system) and a zero temperature/concentration gradient at the outlet.

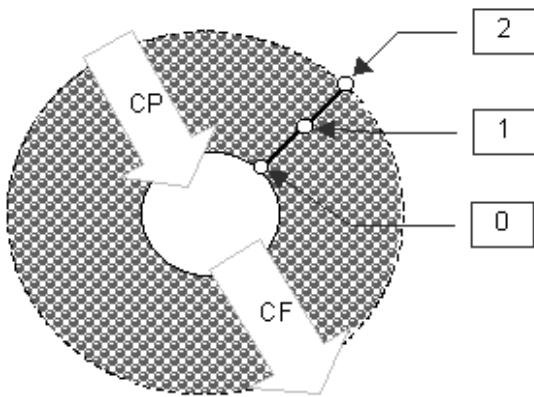
2.2 Derivation of a simplified model

For a simplification of the governing equations, the Lewis-Number (Le) is assumed to be unitary. This also implies that, by definition, the Peclet-Numbers (Pe) for mass and energy are equal: $Pe_M = Pe_H = Pe$. The derivation is presented in Appendix A. With this simplification, the mass and energy governing equations can be combined into a *single* equation, Equation (5), with the invariant defined by Equation (6). This invariant relates the temperature rise to the conversion in steady-state adiabatic reactors.

$$\frac{1}{Pe} \left[\frac{d^2\theta}{d\xi^2} + \frac{a}{\xi} \frac{d\theta}{d\xi} \right] \mp \frac{1}{\xi^a} \frac{d\theta}{d\xi} = -B Da \hat{r}(Y, \theta) \exp\left(\frac{\theta}{1+\theta/\gamma}\right) \quad (5)$$

$$\theta + BY = B \quad (6)$$

2.3 Derivation of the Lumped Model



The numerical solution of the simplified model of this reactor is accomplished using equally spaced finite differences utilizing only three grid points. Two grid points are at the boundaries ("2" & "0") of the reactor bed and one point ("1") is in the middle of the bed, as seen in Figure 3.

Figure 3: Schematic of the cylinder with internal grid-points and utilized coordinates

The governing equation is therefore approximated as Equation (7):

$$\frac{1}{Pe} \left[\frac{\theta_{i+1} - 2\theta_i + \theta_{i-1}}{\Delta\xi^2} + \frac{a}{\xi_i} \left(\frac{\theta_{i+1} - \theta_{i-1}}{2\Delta\xi} \right) \right] \pm \frac{1}{\xi_i^a} \left(\frac{\theta_{i+1} - \theta_{i-1}}{2\Delta\xi} \right) = -B Da \hat{r}(Y, \theta)_i \exp\left(\frac{\theta_i}{1+\theta_i/\gamma}\right) \quad (7)$$

With $i=1$ (total of three grid points, one internal grid point) one arrives at Equation (8):

$$\frac{1}{Pe} \left[\frac{\theta_2 - 2\theta_1 + \theta_0}{\Delta\xi^2} + \frac{a}{\xi_1} \left(\frac{\theta_2 - \theta_0}{2\Delta\xi} \right) \right] \pm \frac{1}{\xi_1^a} \left(\frac{\theta_2 - \theta_0}{2\Delta\xi} \right) = -B Da \hat{r}(Y, \theta)_1 \exp\left(\frac{\theta_1}{1+\theta_1/\gamma}\right) \quad (8)$$

Utilizing the boundary conditions, the temperatures θ_0 and θ_2 can be expressed in terms of θ_1 as shown in Appendix B. Therefore the governing equation of the system is a function of the single parameter θ_1 , the temperature in the middle of the bed. This approximation with a single internal grid point will be used in all derivations and results for the remainder of the paper.

2.4 Reactor Arrangement

Catalytic beds and heat exchangers can be arranged in different ways, as shown before. For this study we will utilize the Haldor-Topsoe S-200[®] converter as a guideline. As seen in Figure 2, the S-200 series consists of two reactor beds with a so-called "inter-bed" heat exchanger and an optional second heat exchanger ("lower heat exchanger"). The heat exchanger is modeled as shown in Figure 4:

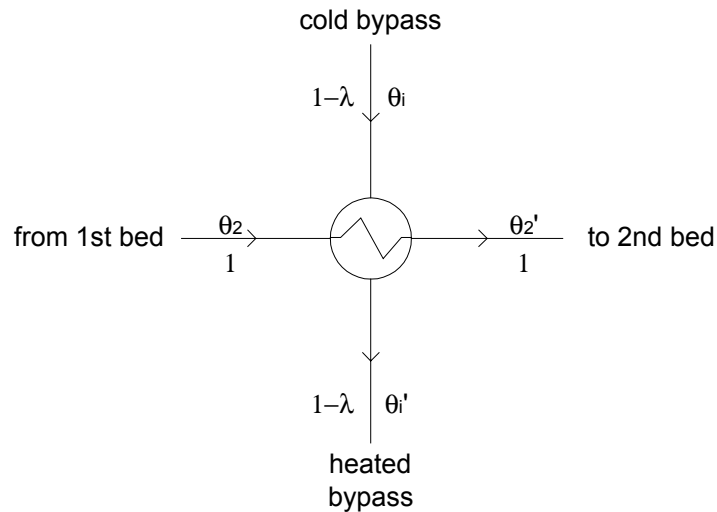


Figure 4: Setup of the inter-bed heat exchanger

The heat exchanger is assumed to have no dynamic delay and a co-current flow configuration. Furthermore, it is assumed that the densities and heat capacities of both streams are equal. An ideal heat exchanger with 100% efficiency will exhibit the temperature profiles shown in Figure 5:

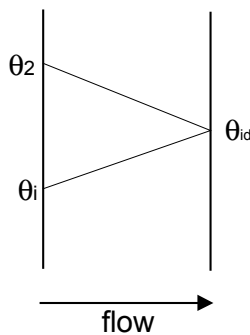


Figure 5: Profiles of heat exchanger

With the assumption of constant densities and heat capacities, the energy balance equation can then be written in terms of temperature differences as:

$$(1 - \lambda)(\theta_{id} - \theta_i) = (\theta_2 - \theta_{id}) \quad (9)$$

which can be easily solved for θ_{id} as,

$$\theta_{id} = \frac{\theta_2 + (1 - \lambda)\theta_i}{(1 - \lambda) + 1} \quad (10)$$

Introducing a heat-exchanger efficiency, ϵ_{HE} , one can solve for both outlet temperatures as,

$$\theta_i' = \epsilon_{HE} \theta_{id} \quad (11)$$

$$\theta_2' = (1 - \epsilon_{HE})\theta_2 + \epsilon_{HE} \theta_{id} \quad (12)$$

where,

ε_{HE} : Efficiency of the heat exchanger

θ_{id} is the outlet temperature for 100% efficiency

$1 - \lambda$: ratio of by - pass flow rate to total inlet flow rate

The second (“lower”) heat exchanger is modeled in an analogous fashion. The additional equations are provided by the mixing points (Equation 13), i.e.,

$$\sum_i \frac{\text{property}(\text{inlet}_i) * \text{flowratio}_i}{\text{total flow}} = \sum_i \frac{\text{property}(\text{outlet}_i) * \text{flowratio}_i}{\text{total flow}} \quad (13)$$

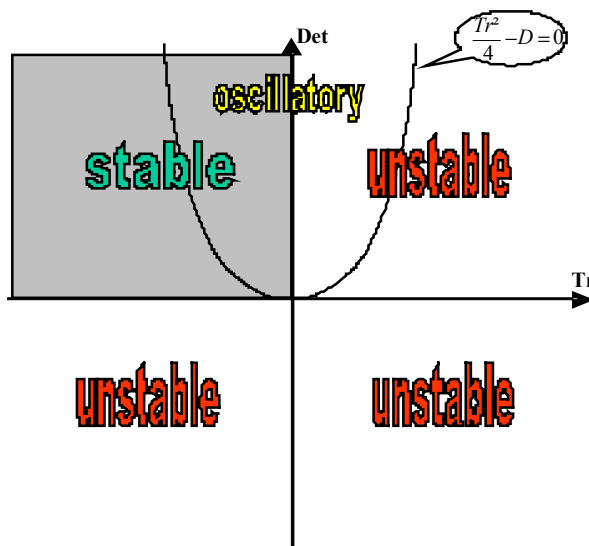
2.5 Stability Analysis

Although not a sufficient condition, the existence of multiple steady states (MSS) is a necessary condition for unstable behavior. In order to draw conclusions about the stability of the obtained steady states, one has to introduce a dynamic analysis of the system. The steady state governing equation (Equation 5) for each reactor “i” can then be formulated as:

$$F_i(\theta_1) = \frac{d\theta_1^i}{dt} = -c_1\theta_1^i + B Da^i R(\theta_1^i) \quad (14)$$

with, $R(\theta_1^i) = \hat{r}(Y, \theta)|_1^i \exp\left(\frac{\theta_1^i}{1 + \theta_1^i / \gamma}\right)$ and $c_1 = f(Pe, \xi_0, a)$

In the following a linear stability analysis of the steady state solution will be performed. The dynamics of finite temperature differences is then determined by the eigenvalues of the Jacobian matrix, $\partial F^i / \partial \theta_1^i$. A convenient way of analyzing the stability of these systems is to plot the determinant, trace and discriminant ($\text{Tr}^2 - 4D$) of the Jacobian of the linearized system, as demonstrated in Figure 6.



From such a plot, one can quickly assess the different regions of stability. It is a well-known fact that only a system with positive values of the determinant and negative trace will exhibit stable behavior. In addition one can classify the dynamics as node-like if the discriminant is positive, while for negative values the system will exhibit a focus-like behavior.

One important drawback for the simplified system represented by the lumped model is the inability to capture oscillatory behavior for a configuration with a single inter-bed heat exchanger. Indeed, since this system will not exhibit a feedback from the second bed, the off-diagonal element of the Jacobian will always be zero and imaginary roots cannot occur.

Figure 6: Stability Regions for a two-dimensional system

3. RESULTS

3.1.1 Steady State Solution and Multiplicity Regions without heat exchange

In the following, the steady-state solutions corresponding to a single bed and to two different multiple-bed configurations are shown. Solving a single catalytic bed, as shown in Figure 7, one obtains the following locus of steady state solutions for the given set of operating parameters.

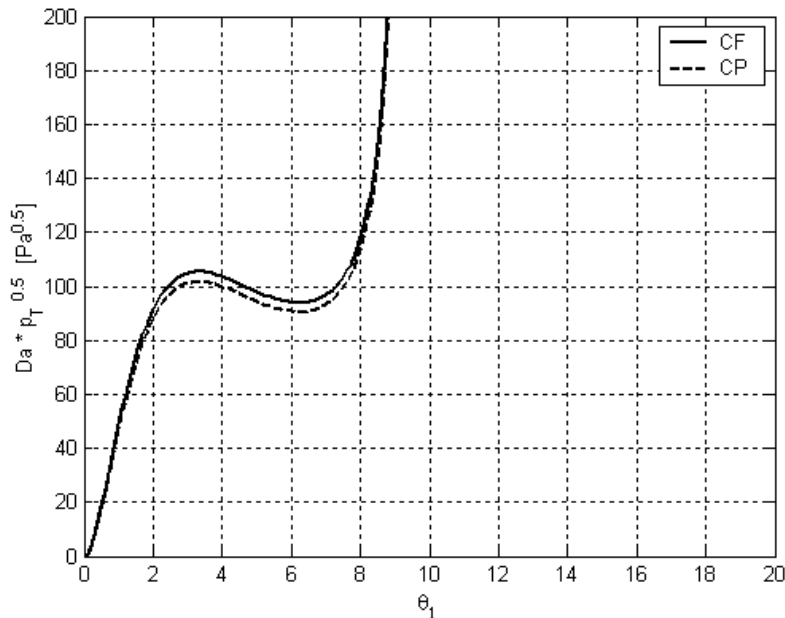


Figure 7: Steady-State Solution for a single bed (utilized parameters: $B=20$, $Pe=10$, $\epsilon=0.05$, $\xi_0=0.5$, $a=1$, CF/CP flow, $p_T=200\text{bar}$, $K=1e-14$)

Figure 7 depicts the characteristic S-shaped curve steady-state solution, indicating the existence of multiple steady states (multiplicity) for a certain range of the Damköhler number, Da . The system can, depending on Da , exhibit one, two or three different steady states. The influence of the flow direction, either centripetal (CP) or centrifugal (CF), is observed. One can see that the effect of the flow direction is not very important; this effect, however, might be masked in this model by the assumption of constant total pressure.

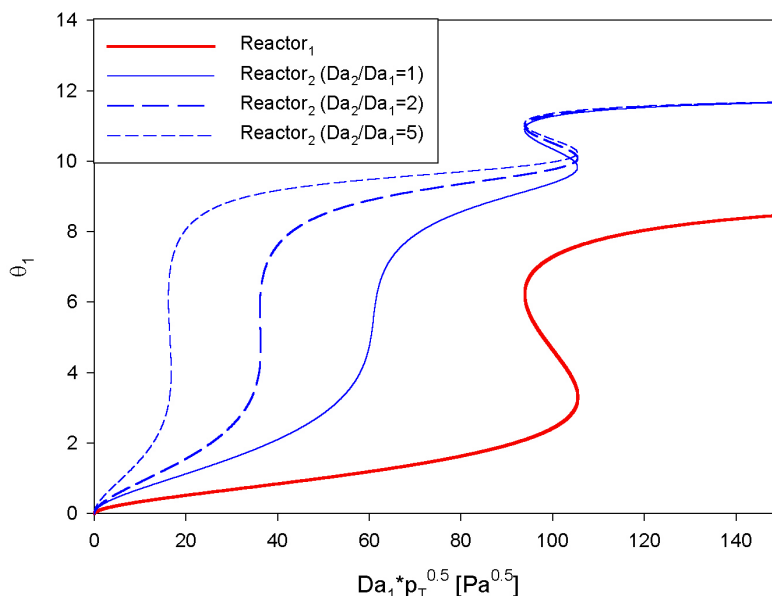


Figure 8: Two reactors in series, no heat exchange (utilized parameters: $B=20$, $Pe=10$, $\epsilon=0.05$, $\xi_0=0.5$, $a=1$, CF flow, $p_T=200\text{bar}$, $K=1e-14$)

Figure 8 shows the solutions of a setup with 2 reactors in series and no heat exchange. From this figure, one can observe the same multiplicity behavior of the first reactor as seen in Figure 7. For an equal-sized second reactor the solution shows that multiplicity at the upper solution branch of the second reactor only occurs due to the multiplicity behavior in the first reactor. However, increasing the size ratio (Da_2/Da_1) one can see that for a limiting case of (Da_2/Da_1)=2 the second reactor exhibits multiplicity independent from the first reactor. Furthermore, one can note that beyond a certain point on the upper branch the solutions of

different size ratios coincide. This occurs due to equilibrium limitations.

3.1.2 Combination of two beds with one interbed heat exchanger

Combining two catalyst beds with an inter-bed heat exchanger now opens a wider window of solutions. Since every reactor can exhibit up to three different solutions, the system of two catalyst beds in series will exhibit up to a maximum of nine possible steady states. The spectrum of solutions now depends both on the individual Damköhler numbers, Da , and the cooling between the reactors. However, the fact that the cooling is not independent, but limited due to the feedback, will limit the number of possible steady states of the system.

A very simple and important mechanism to control the reactor performance is by varying the flow ratios of the different streams of the system. In the following the effect of the bypass is demonstrated.

Figure 9 and Figure 10 show how the parameter “ λ ”, the fraction of reactants, which enters the reactor without preheating (cf. Figure 2), changes the state profile of the system.

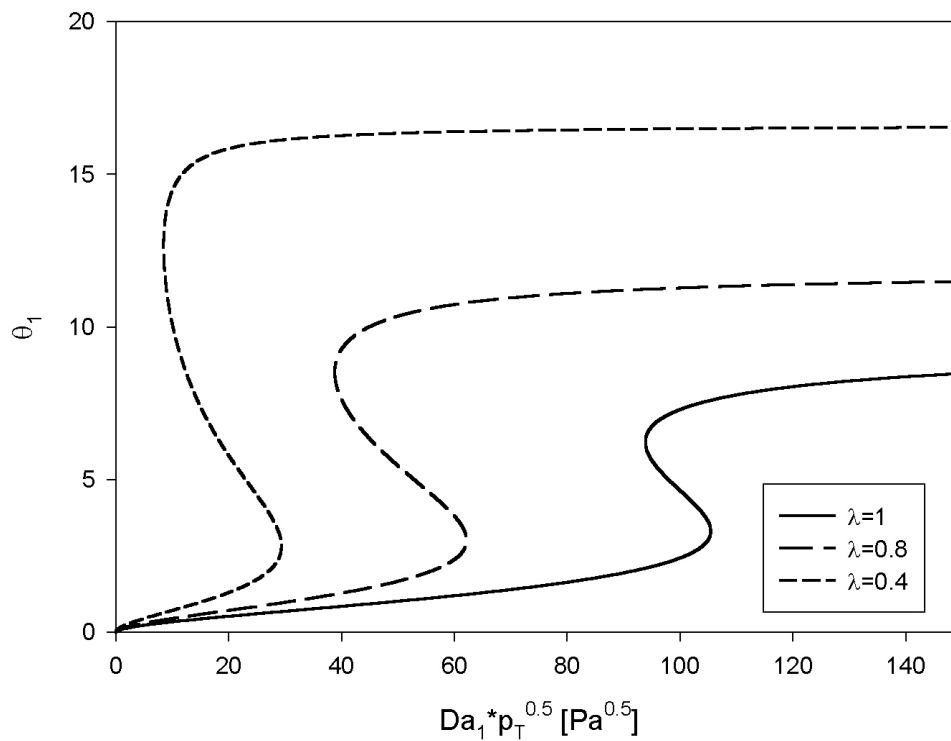


Figure 9: Effect of the flow ratios on the steady state solution in terms of temperature in the first reactor (utilized parameters: $B=20$, $Pe=10$, $\varepsilon=0.05$, $\xi_0=0.5$, $a=1$, CF flow, $p_T=200\text{bar}$, $K=1\text{e-}14$)

Figure 9 and Figure 10 show how decreasing values of λ lead to a much flatter steady state profile. This also shifts the solutions to higher temperatures. Since the amount of reactants bypassed and preheated increases, so does the temperature in the reactor, leading to the flatter and stretched profile. The important point to notice is, in other words, that through decreasing λ one can achieve the same temperature or concentration difference with a smaller Da .

For any control purposes one also should be aware of the quite drastic change in the shape of the profiles imposing a potentially strong dynamics on the controller.

In the following, the effect of the preheating of reactants is demonstrated in terms of the flow ratio λ :

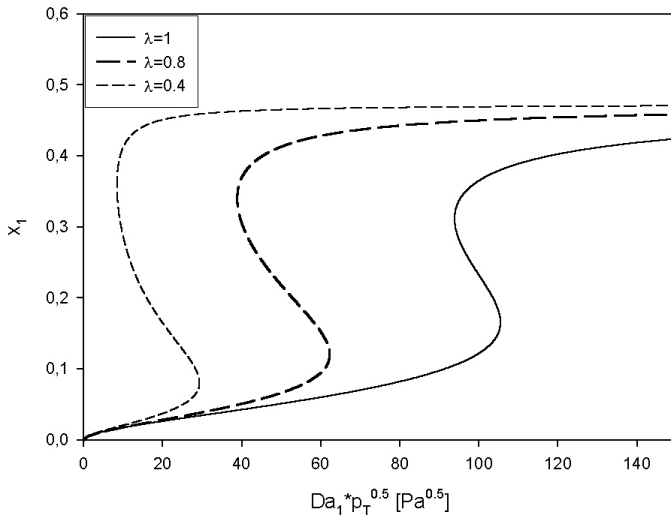


Figure 10: Effect of the flow ratios on the steady state solution in terms of conversion in the first reactor (utilized parameters: $B=20$, $Pe=10$, $\varepsilon=0.05$, $\xi_0=0.5$, $a=1$, CF flow, $p_T=200\text{bar}$, $K=1e-14$)

Figure 11 shows the solutions obtained for different values of Da with varying λ . For large Damköhler-Number (125) one can see that the reactor operates at the upper steady state only. A decrease in λ , which relates to pre-heating the feed through the first heat exchanger, leads to increasing reactor temperature. For lower values of Da , however, one can observe that an increase in the pre-heated flow (i.e. decreasing λ) leads to multiplicity. For a Damköhler Number of 30, for example, the reactor would ignite once λ is decreased below 0.4. As the Damköhler Number decreases, the system eventually reaches a limiting condition (for the example, Damköhler Number, $Da=17$) below which the reactor will not ignite by means of manipulating λ . Other solutions at higher temperatures still exist, but would only be realized in cases where the reactor is subject to a large perturbation.

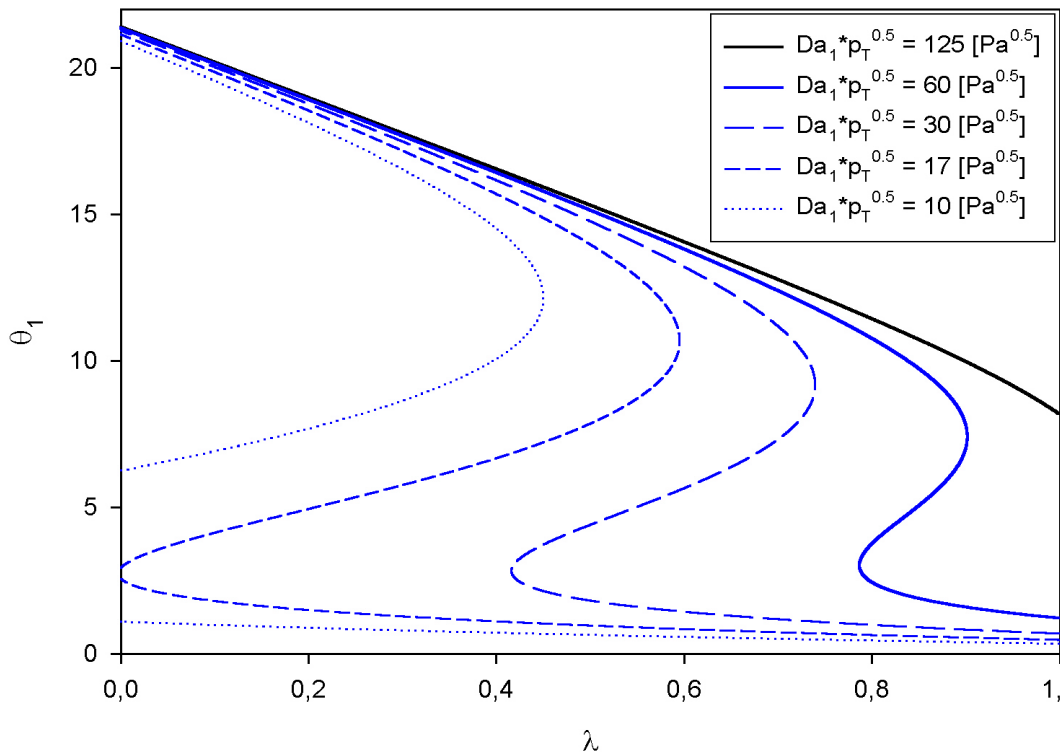


Figure 11: Temperature profiles in dependence of λ for various Da (utilized parameters: $B=20$, $Pe=10$, $\varepsilon=0.05$, $\xi_0=0.5$, $a=1$, CF flow, $p_T=200\text{bar}$, $K=1e-14$)

In principle, this observed behavior also holds for the setup with two heat exchangers. However, since visualization in this case is difficult due to an additional parameter (flow ratio μ_2), the analysis has been limited to a single heat-exchanger configuration.

Comparing these results with those reported by Pedernera et al. (1999) (cf. Figure 12) one can see that the lumped model qualitatively exhibits the same behavior, clearly identifying the effect of the bypass on the process multiplicity.

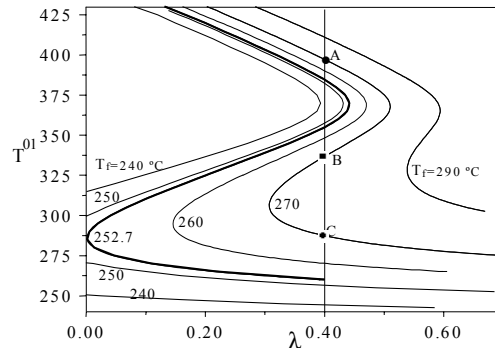


Figure 12: Effect of λ according to Pedernera et al. (1999)

3.1.3 Combination of two beds with two heat exchangers

For the combination of two reactors with two heat exchangers (cf. Figure 2), The locus for the steady-state solutions changes significantly, as shown in Figure 13.

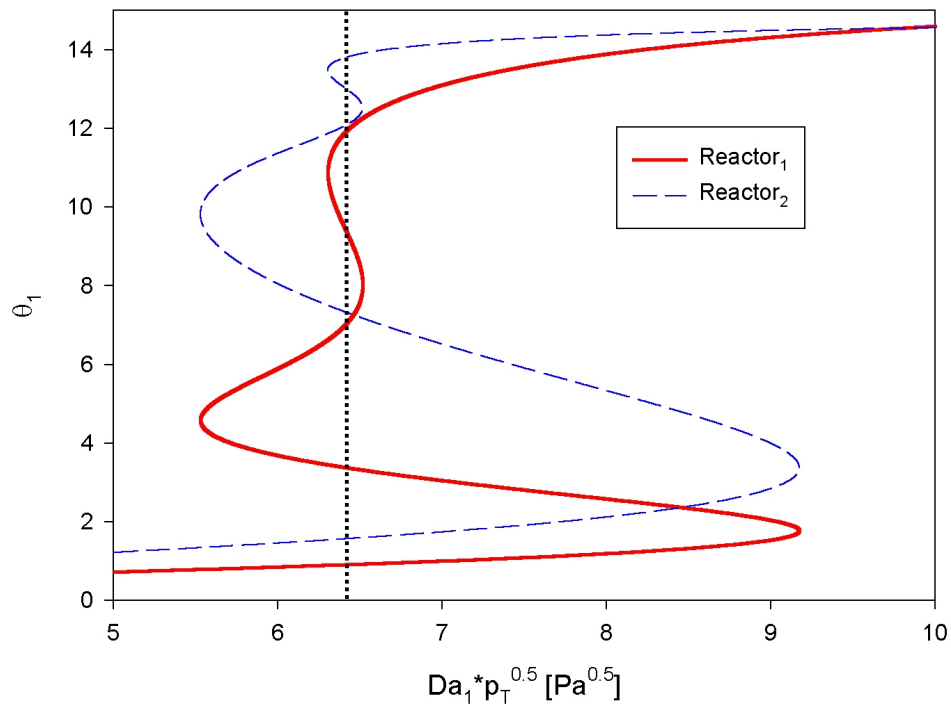


Figure 13: Steady-State Solution for the arrangement with two heat exchangers ($B=20$, $Pe=10$, $\varepsilon=0.05$, $\xi_0=0.5$, $a=1$, CF flow, $p_1=200\text{bar}$, $K=1e-14$, $Da_2/Da_1=4$, $\lambda=0.5$, $\mu_1=\mu_2=0.25$)

The locus for the steady-state solutions still shows the typical S-shape. This profile, however, is significantly extended. In addition, a smaller multiplicity (S-shaped) region is observed in the higher temperatures range. Here the system will exhibit five (5) possible steady state solutions.

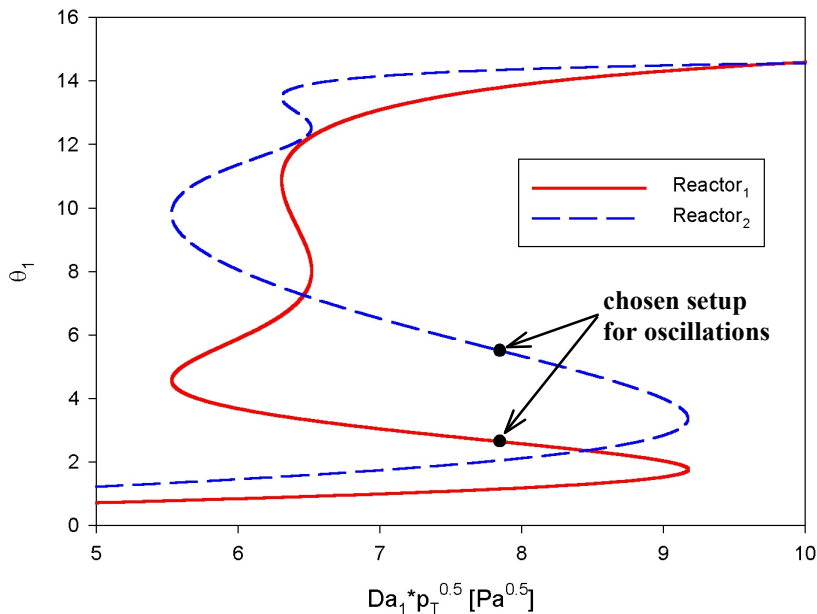


Figure 14: Chosen setup for an oscillating system ($B=20$, $Pe=10$, $\varepsilon=0.05$, $\xi_0=0.5$, $a=1$, CF flow, $p_T=200\text{bar}$, $K=1e-14$, $\lambda=0.5$, $\mu_1=\mu_2=0.25$, $(Da_2/Da_1)=4$)

these data were obtained for unknown operating conditions, our results cannot be compared directly with that reference. It is, however, worth noticing that the behavior predicted by the simplified model bears a strikingly similar dynamics, highlighting its potential for establishing control strategies.

For the system with both heat exchangers, the lumped model is capable of identifying the conditions for oscillatory behavior.

As shown in Figure 14, one can observe sustained oscillations in the system. The temperatures in each bed related to each other are shown in the phase plane depicted in Figure 15, with the transient temperature shown as well. One can see that the first reactor has a phase shift compared to the second reactor.

Oscillatory behavior has been observed in an industrial ammonia converter as shown by Morud and Skogestad (1998). Since

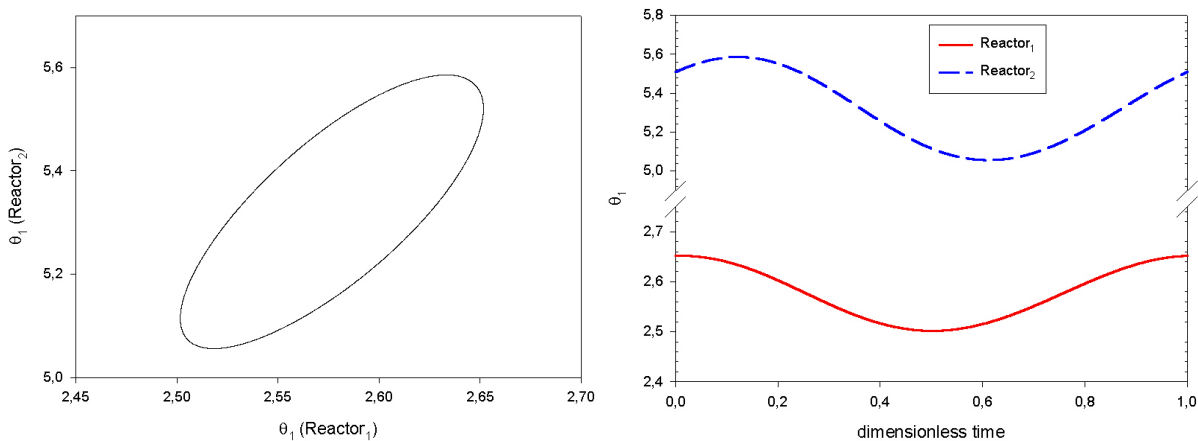


Figure 15: Phase plot and transient temperature of the obtained oscillations

3.2 Temperature Profiles

The model presented in this work has been proposed in the light of computational simplicity, ultimately favorable for real time evaluation of the governing equations.

In the following, temperature and conversion profiles for a particular reactor configuration and a selected set of operating conditions, will be qualitatively compared with the results obtained from a detailed heterogeneous model effort presented by Pedernera et al. (1999). Figures 16 and 17 show the temperature and conversion profiles reported by Pedernera et al. (1999):

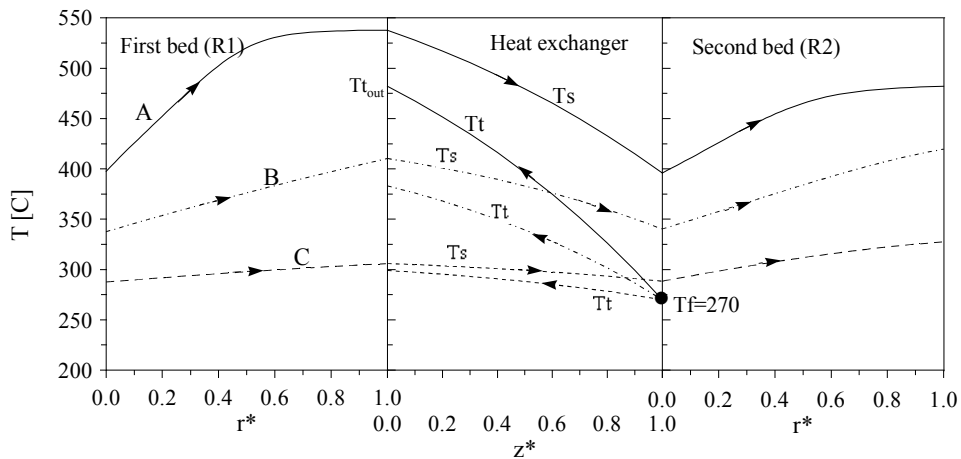


Figure 16: Temperature profiles of the heterogeneous model from Pedernera et al. (1999)

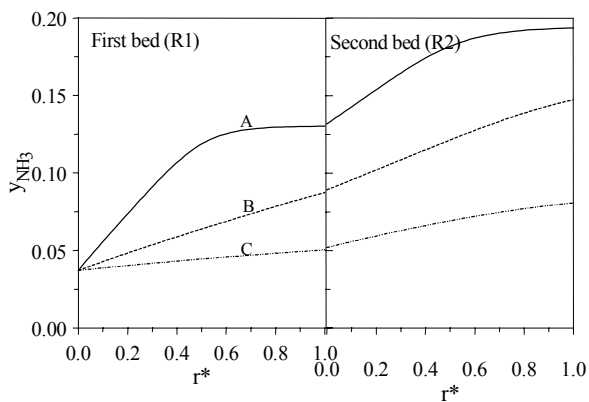


Figure 17: Conversion profiles of the heterogeneous model from Pedernera et al. (1999)

Table 1: Operating parameters for the obtained profiles

Reactors	Flow ratios
$Da_1^*(p_T^{0.5})=40 Pa^{0.5}$	$\lambda=0.8$
$Da_2^*(p_T^{0.5})=80 Pa^{0.5}$	$\mu_1=\mu_2=0.1$

The comparison corresponds to the two heat-exchangers configuration, as shown in Figure 2. The operating parameters are listed in Table 1. Figures 18 and 19 show the temperature and conversion profiles for the simplified model. Since (ideal) heat exchangers with purely linear profiles are

assumed, the temperature profiles of the heat exchangers have not been included. The temperatures at the outlet of the first reactor and the entrance of the second reactor do not coincide, due to the presence of a heat exchanger that lowers the temperature between the reactors, as well as due to the fact that the Danckwerts' boundary conditions lead to a discontinuity at the reactor inlet. For the case of the conversion profiles, this discontinuity is due to the Danckwerts boundary conditions.

The presented temperature and conversion profiles are 2nd order polynomials based on the three temperatures obtained from the governing equation and boundary conditions.

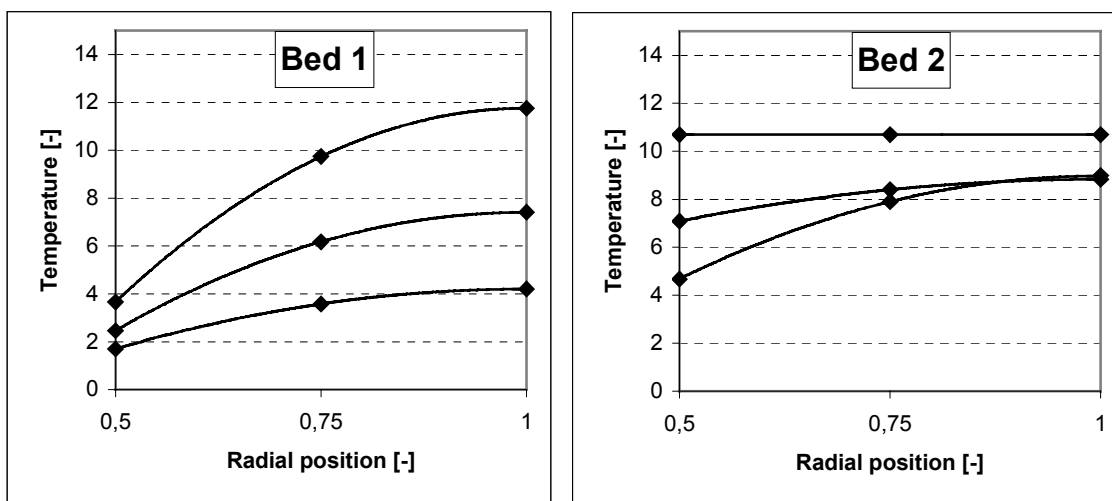


Figure 18: Temperature profiles of the presented model for both beds

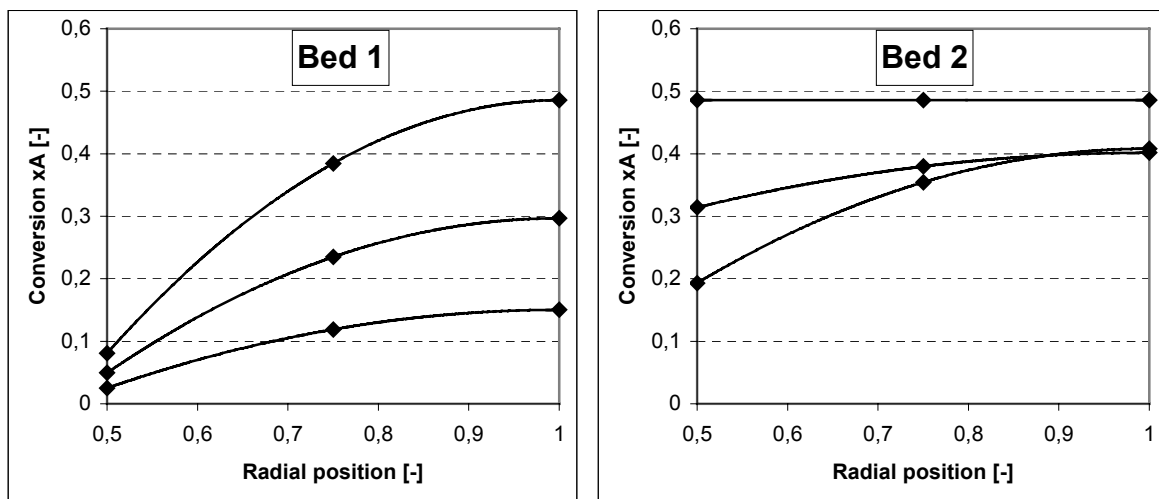


Figure 19: Conversion profiles of the presented model for both beds

In accordance to the Danckwerts' boundary conditions, the temperature and conversion profiles present the characteristic discontinuity at the inlet and the zero-derivative (of temperature or conversion with respect to position) at the outlet.

The comparison between the reported profiles highlights the fact that high conversion profiles obtained from the heterogeneous model have a slower increase towards the end of the bed. This effect might be due to a different equilibrium condition in the reactor. These types of effects cannot be captured by the simplified model due to its discrete nature. Furthermore, the effect of equilibrium limitations in the second bed become also apparent in the configuration under analysis. When the reaction reaches high temperatures, it will therefore also reach its equilibrium limits which will prohibit further temperature and conversion rise, with the profiles corresponding to the upper state resulting in flat temperature or concentration profiles (i.e., constant). However, one has to note that the equilibrium constant used in this work differs from that used by Pedernera et al. (1999). A comparison between the heterogeneous model presented by Pedernera et al. (1999) with the lumped model shows that the temperature and

conversion profiles are in qualitative agreement. However, in contrast to the much more complex heterogeneous model, all the profiles in the lumped model are obtained via a simple 2nd order polynomial based on 3 finite points.

4. CONCLUSIONS AND SUMMARY

A simplified reduced-order model for two different autothermal radial flow reactor arrangements has been developed. From the steady-state solution of a single bed one can observe that the model still captures the multiplicity (see Figure 7) exhibited by fixed-bed reactors. The presence of multiplicity predicted by the model is also consistent with qualitative changes in all parameters.

Multiplicity of steady states was observed for a single reactor as well as multiple reactor(s) - heat exchanger(s) setups. It has been shown how different ratios of the Damköhler Number change the multiplicity behavior (Figure 8). In the (second) setup including two feedback loops, one also can observe a case of five (5) possible steady states for certain combinations of Damköhler Numbers (Figure 13). This suggests that autothermal setups exhibit even a wider range of solutions.

The effect of the bypassing (preheating reactants) has also been demonstrated (Figure 9). Preheating of the reactants leads to rather drastic changes of the state profiles. This reflects a potential strong dynamics of the system, which is especially important in the light of implementing control strategies. Furthermore, it has been shown (Figure 11) how the feedback mechanism influences the multiplicity behavior. It is possible to either ignite or extinguish the reactor by changing the by-pass flow ratio, “ λ ” (cf. Figure 2). This result is in agreement with those reported by Pedernera et al. (1999) in a previous contribution.

A stability analysis based on a perturbation of the steady state solution has been performed. This analysis reveals that the states will all be either stable (focus) or unstable (focus) for the arrangement with a single heat exchanger. No node- or oscillatory behavior can be observed due to the missing feedback from the second reactor. It has been demonstrated, on the other hand, that the reactor setup with two heat exchangers indeed exhibits oscillatory behavior (cf. Figures 14 and 15). Furthermore, a dynamic stability analysis, also based on a perturbation from the steady state, showed the stable and unstable operating points.

In addition, a qualitative comparison of the temperature and conversion profiles with those calculated from detailed models (Pedernera et al., 1999) showed qualitative agreement despite the simplified nature of the lumped model.

Since the developed model is of a simplified nature, it is advantageous for real-time evaluation in control applications. Controlling this kind of reactor setup can be achieved by controlling the flow rates of reactants directly fed to the first reactor and reactants preheated by either the first or second heat exchanger. Based on the developed model, an approach to control the reactor utilizing Cell-to-cell Mapping, a novel computational tool for a global analysis of nonlinear dynamic systems, was presented by Chen et al. (2002) and it will be the subject of a forthcoming contribution.

Further research includes the stability analysis for the system with two heat exchangers in a more detailed fashion. So far the analysis revealed stable behavior for positive slopes in the Da - temperature state space and unstable behavior for negative slopes as shown in classical stability analysis by van Heerden (1958). Furthermore the effect of the simplifying assumptions should be investigated. This could reveal if some of the assumptions can be eliminated without increasing the complexity of the model above certain critical levels.

ACKNOWLEDGEMENTS

Financial support from the Established Full-time Faculty Research Development (EFFRD) program at Cleveland State University (CSU) is gratefully acknowledged. Financial support and technical facilities from the Department of Chemical and Biomedical Engineering at CSU were also essential in completing this research and are acknowledged. One of the authors, Malte Bartels, would like to thank the Fulbright Association for their partial support within a student exchange program.

NOTATION

- B dimensionless adiabatic temperature rise, $B = \frac{-\Delta h_R c^*}{\rho_G c_P} \frac{\gamma}{T} = \Delta T_{ad} \frac{\gamma}{T}$ [-]
- c_i concentration of component i $\left[\frac{\text{mol}}{\text{m}^3} \right]$
- c_P spec. heat capacity (at const. pressure) $\left[\frac{\text{J}}{\text{kg K}} \right]$
- D Diffusioncoefficient / mass diffusivity $\left[\frac{\text{m}^2}{\text{s}} \right]$
- Da Damköhler number, $Da = \frac{R^*}{u^*} \frac{1}{c^*} k_0 e^{-\gamma} p_T^{(1+order)}$ [-]
- E Activation Energy $\left[\frac{\text{J}}{\text{mol}} \right]$
- $-\Delta h_R$ spec. heat of reaction $\left[\frac{\text{kJ}}{\text{kmol}} \right]$
- $-\Delta h_R^\circ$ spec. heat of reaction (Standardconditions) $\left[\frac{\text{kJ}}{\text{kmol}} \right]$
- k_0 preexponential factor $\left[\frac{\text{kmol}_{NH_3}}{\text{Pa}^{(1+order)} \text{m}^3 \text{h}} \right]$
- k_1 spec. Reactionrate Forwardreaction (acc. to Temkin - Pyzhev) $\left[\frac{\text{kmol}_{NH_3}}{\text{Pa}^{3/2} \text{m}^3 \text{h}} \right]$
- k_2 spec. Reactionrate Backwardreaction (acc. to Temkin - Pyzhev) $\left[\frac{\text{kmol}_{NH_3}}{\text{Pa}^{-1/2} \text{m}^3 \text{h}} \right]$
- K Equilibriumconstant for Temkin - Pyzhev - Kinetics, $K = \frac{k_1}{k_2} [\text{Pa}^{-2}]$
- Le Lewis - Number, $Le = \frac{Pe_H}{Pe_M} = \frac{D}{\alpha}$ [-]
- $order$ Reactionorder (acc. to Temkin - Pyzhev - Kinetics expression 0.5) [-]
- p_i partial pressure of component i [Pa]
- p_T total pressure of reactor [Pa]
- Pe_H Peclet - Number for Heat, $Pe_H = \frac{u^* R^*}{\alpha}$ [-]
- Pe_M Peclet - Number for Mass, $Pe_M = \frac{u^* R^*}{D}$ [-]
- r radius [m]
- \hat{r} dimensionless reaction rate : $\hat{r}(Y, \theta) = \left[y_A \left(\frac{y_B^3}{y_C^2} \right)^{0.5} - \frac{1}{K} p_T^{-2} \left(\frac{y_C^2}{y_B^3} \right)^{0.5} \right]$
- R radius for borders (see indices!) [m]

t	Time [s]
T	Temperature [K]
ΔT_{ad}	adiabatic Temperature rise, $\Delta T_{ad} = \frac{-\Delta h_R c^*}{\rho_G c_P} [K]$
u	velocity of fluid $\left[\frac{m}{s} \right]$
x_i	conversion of component i [-]
y_i	molar fraction of component i [-]
y_{i0}	initial molar fraction of component i [-]
Y	dimensionless concentration, $Y = \frac{c}{c^*} [-]$

Greek letters:

α	thermal diffusivity, $\alpha = \frac{\lambda_{Th}}{\rho_G c_P} \left[\frac{m^2}{s} \right]$
Δ	Difference, $\Delta \xi = \xi_{i+1} - \xi_{i-1}$
ε	inverse of dimensionless activation energy: $\varepsilon = 1/\gamma [-]$
ε_{HE}	Efficiency of the heat exchanger [-]
λ_{Th}	thermal conductivity $\left[\frac{J}{s m K} \right]$
λ	flow ratio not bypassed [-]
μ_i	flow ratio bypassed (see flow sheet) [-]
γ	dimensionless activation energy, $\gamma = \frac{E}{RT^*} [-]$
ω_i	Reactionrate of component i, $\omega_i = \frac{dc_i}{dt} \left[\frac{mol}{m^3 s} \right]$
ρ_{cat}	density of the catalyst $\left[\frac{kg}{m^3} \right]$
ρ_G	density of the gaseous reactants $\left[\frac{kg}{m^3} \right]$
θ	dimensionless Temperature, $\theta = \frac{T - T^*}{T^*} \gamma [-]$
θ'	derivative of dimensionless Temperature, $\theta' = \frac{d\theta}{d\xi} [-]$
ξ	dimensionless radius, $\xi = \frac{r}{R^*} [-]$

Indices:

- * Reference state (Definition depends on the application!)
- 0 position at inner surface of hollow catalyst - cylinder
- 1 position in the middle of hollow catalyst - cylinder
- 2 position at outer surface of hollow catalyst - cylinder

Subscripts refer to the position along the radial coordinate. The superscript refers to the reactor in the sequence.

REFERENCES

- Aabashar, M.E.E., "Application of heat interchange systems to enhance the performance of ammonia reactors", *Chem. Eng. Journal*, Vol. 78, 69-79 (2000)
- Bildea, C.S., Dimian, A.C., Iedema, P.D., "Multiplicity and stability approach to the design of heat-integrated multibed plug-flow reactor", *Comp. & Chem. Eng.*, Vol. 25, 41-48 (2001)
- Chen, Z.Z., Ungarala, S., Bartels, M., Gatica, J., Pedernera, M.N., Schbib, N.S., "Control and Stability Analysis of Autothermal Radial Flow Reactors using Reduced-Order Models", Annual AIChE-Meeting (Indianapolis, Indiana), Session 280g (2002)
- Dankwerts, P.V., "Continuous Flow Systems – Distribution of Residence Times", *Chemical Engineering Science*, Vol. 2, No. 1, 1-18 (1953)
- Fogler, S., "Elements of Chemical Reaction Engineering", 3rd edition, Prentice Hall PTR (1999)
- Hairston, D., "Chemical Engineering" (edited by Deborah Hairston), Vol. 11, 27-32 (2002)
- Hlavacek, V., Kubicek, M., "Modeling of chemical reactors – XXV Cylindrical and spherical reactor with radial flow", *Chemical Engineering Science*, Vol. 27, 177-186 (1972)
- Kienle, A., Lauschke, G., Gehrke, V., Gilles, E.D., "On the dynamics of the circulation loop reactor – numerical methods and analysis", *Chem. Eng. Sci.*, Vol. 50, No. 15, 2361-2375 (1995)
- Kolios, G., Frauhammer, J., Eigenberger, G., "Autothermal fixed-bed reactor concepts" (Review), *Chem. Eng. Sci.*, Vol. 55, 5945-5967 (2000)
- Morud, J.C., Skogestad, S., "Analysis of instability in industrial ammonia reactors", *AIChE Journal*, Vol. 44, 888-895 (1998)
- Pedernera, M.N., Borio, D.O., Schbib, N.S., "Steady State Analysis and Optimization of a Radial-Flow Ammonia Synthesis Reactor", *Comp. & Chem. Eng.*, S773-S776 (1999)
- Slack, A.V., James, G.R., "Fertilizer science and technology series – Volume2 : Ammonia (Part I & III)", edited by A.V. Slack & G. Russell James, Marcel Dekker Inc. (1977)
- Strelzoff, S., "Technology and Manufacture of Ammonia", John Wiley&Sons (1981)
- Temkin, V.I., Pyzhev, V., "Kinetics of Ammonia Synthesis on Promoted Iron Catalysts", *Acta Physicochimica (U.R.S.S.)*, Vol. 12, No. 3, 327-356 (1940)
- Ullmann's Encyclopedia, Ullmann's Encyclopedia for Industrial Chemistry, 5th edition, Vol. A2, p. 193, VCH, (1993)
- van Heerden, C., "The character of the stationary state of exothermic processes", *Ind. Eng. Chem.*, Vol. 45, 1242-1247 (1958)
- Vancini, C.A., "Synthesis of Ammonia", MacMillan (1971)
- Vortmeyer, D., Schaefer, R.J., "Equivalence of One- and Two-Phase Models for Heat Transfer Processes in Packed Beds: One Dimensional Theory", *Chem. Eng. Sci.*, Vol. 29, 485-491 (1974)

APPENDICES

Appendix A: Derivation of a Simplified Model assuming $Le=1$

For a simplification of the governing equations the Lewis-Number is assumed to be unitary. This also indicates by definition that the Peclet-Numbers are equal ($Pe_M=Pe_H=Pe$). As shown above, the dimensionless mass and energy balances are:

Mass Balance

$$\frac{1}{Pe_M} \left[\frac{\partial^2 Y}{\partial \xi^2} + \frac{a}{\xi} \frac{\partial Y}{\partial \xi} \right] \pm \frac{1}{\xi^a} \frac{\partial Y}{\partial \xi} = Da \exp\left(\frac{\theta}{1+\theta/\gamma}\right) \hat{r}(Y, \theta)$$

Energy Balance

$$\frac{1}{Pe_H} \left[\frac{\partial^2 \theta}{\partial \xi^2} + \frac{a}{\xi} \frac{\partial \theta}{\partial \xi} \right] \pm \frac{1}{\xi^a} \frac{\partial \theta}{\partial \xi} = -B Da \exp\left(\frac{\theta}{1+\theta/\gamma}\right) \hat{r}(Y, \theta)$$

subject to the boundary conditions (according to Danckwerts (1953)):

$$\begin{aligned} \xi = \xi_0 : Pe_M (1 - Y) &= -\xi_0^a \frac{\partial Y}{\partial \xi} & \xi = \xi_0 : Pe_H \theta &= -\xi_0^a \frac{\partial \theta}{\partial \xi} \\ \xi = \xi_2 : \frac{\partial Y}{\partial \xi} &= 0 & \xi = \xi_2 : \frac{\partial \theta}{\partial \xi} &= 0 \end{aligned}$$

Multiplying the mass balance by the dimensionless adiabatic temperature rise, B, and adding both balances, provided that both Peclet numbers are identical ($Pe_M=Pe_H=Pe$), one obtains:

$$\frac{1}{Pe} \left[\frac{\partial^2 (\theta + BY)}{\partial \xi^2} + \frac{a}{\xi} \frac{\partial (\theta + BY)}{\partial \xi} \right] \pm \frac{1}{\xi^a} \frac{\partial (\theta + BY)}{\partial \xi} = 0$$

In other words, the invariant

$$\theta + BY = \text{constant}$$

is identified. This derivation can be completed if we resort to the boundary conditions, and combine them using the same approach, i.e. (shown for CF, however the same holds for CP):

$$\begin{aligned} \text{at } \xi = \xi_0 : \\ \xi_0^a \frac{\partial (\theta + BY)}{\partial \xi} &= Pe * (\theta - B + BY) \end{aligned}$$

in other words,

$$\theta + BY = B$$

In summary the system can be represented by a single equation,

$$\frac{1}{Pe_H} \left[\frac{\partial^2 \theta}{\partial \xi^2} + \frac{a}{\xi} \frac{\partial \theta}{\partial \xi} \right] \pm \frac{1}{\xi^a} \frac{\partial \theta}{\partial \xi} = -B Da \exp\left(\frac{\theta}{1+\theta/\gamma}\right) \hat{r}(Y, \theta)$$

with: $Y = (1 - \theta / B)$

Note that with these changes now of course also the boundary conditions change accordingly (see Appendix B).

Appendix B: Derivation of a Lumped Model for Multiplicity Analysis

In order to obtain a lumped model for the stability analysis of the system, we first approximate the derivatives with equations in differences. The following derivations are expressed in terms of the indices 0, 1 and 2, i.e. a single internal grid-point. The function for the temperature is then approximated with a 2nd-order polynomial (this is a natural assumption if we follow the method of weighted residuals, for instance)

$$\theta = a + b(r - R_1) + c(r - R_1)^2$$

So one can express the slope of the temperature gradient as the derivative of the dimensionless temperature:

$$\frac{d\theta}{dr} = b + 2c(r - R_1)$$

Writing the temperature-function for all 3 points one gets:

$$\begin{aligned} r = R_0 &\rightarrow \theta_0 = a + b(R_0 - R_1) + c(R_0 - R_1)^2 \\ r = R_1 &\rightarrow \theta_1 = a + b(R_1 - R_1) + c(R_1 - R_1)^2 = a \\ r = R_2 &\rightarrow \theta_2 = a + b(R_2 - R_1) + c(R_2 - R_1)^2 \end{aligned}$$

Solving for the constants “b” and “c”:

$$\begin{aligned} \theta_0 - 2\theta_1 + \theta_2 &= 2c * \Delta r^2 \\ \rightarrow c &= \frac{\theta_0 - 2\theta_1 + \theta_2}{2\Delta r^2} \end{aligned}$$

$$\begin{aligned} \theta_2 - \theta_0 &= 2b * \Delta r \\ \rightarrow b &= \frac{\theta_2 - \theta_0}{2\Delta r} \end{aligned}$$

Solving for the Boundary Conditions, one can show that (θ^0 represents inlet conditions as reference):

Centrifugal (CF) Flow Configuration:

$$r = R_0 : \frac{Pe(\theta_o - \theta^o)}{\xi_o^a} = \frac{-3\theta_0 + 4\theta_1 - \theta_2}{2\Delta \xi}$$

$$r = R_2 : 0 = \frac{\theta_0 - 4\theta_1 + 3\theta_2}{2\Delta\xi}$$

Centripetal (CP) Flow Configuration:

$$r = R_0 : 0 = \frac{-3\theta_0 + 4\theta_1 - \theta_2}{2\Delta\xi}$$

$$r = R_2 : -Pe(\theta_2 - \theta^o) = \frac{\theta_0 - 4\theta_1 + 3\theta_2}{2\Delta\xi}$$

In case of one interior discretization point, the governing equation is written as:

$$\frac{1}{Pe} \left[\frac{\theta_2 - 2\theta_1 + \theta_0}{\Delta\xi^2} + \frac{a}{\xi_1} \left(\frac{\theta_2 - \theta_0}{2\Delta\xi} \right) \right] \mp \frac{1}{\xi_1^a} \left(\frac{\theta_2 - \theta_0}{2\Delta\xi} \right) = -B Da \exp\left(\frac{\theta_1}{1 + \theta_1/\gamma}\right) \hat{r}(Y, \theta)$$

The reduction to a single equation requires one to express θ_0 and θ_2 as functions of θ_1 to arrive at a single equation with the unknown θ_1 . Solving both boundary conditions for the temperatures, one can rewrite the system as:

Centrifugal (CF) Flow Configuration:

$$\theta_0 = \frac{8\theta_1\xi_0^a + 3Pe\theta^o(1 - \xi_0)}{8\xi_0^a + 3Pe(1 - \xi_0)}$$

$$\theta_2 = \frac{\theta_1(-8\xi_0^a + 4Pe\xi_0 - 4Pe) + Pe\theta^o(1 - \xi_0)}{(-8\xi_0^a + 3Pe\xi_0 - 3Pe)}$$

Centripetal (CP) Flow Configuration:

$$\theta_0 = \frac{\theta_1[8 + 4Pe(1 - \xi_0)] - Pe\theta^o(1 - \xi_0)}{8 + 3Pe(1 - \xi_0)}$$

$$\theta_2 = \frac{-8\theta_1 - 3Pe\theta^o(1 - \xi_0)}{-8 - 3Pe(1 - \xi_0)}$$

For reasons of clarity the equations are not combined, but it becomes apparent that the system can now be characterized by a single parameter, “ θ_1 ”.